

REPORT DOCUMENTATION PAGE			Form Approved OMB NO. 0704-0188		
<p>The public reporting burden for this collection of information is estimated to average 1 hour per response, including the time for reviewing instructions, searching existing data sources, gathering and maintaining the data needed, and completing and reviewing the collection of information. Send comments regarding this burden estimate or any other aspect of this collection of information, including suggestions for reducing this burden, to Washington Headquarters Services, Directorate for Information Operations and Reports, 1215 Jefferson Davis Highway, Suite 1204, Arlington VA, 22202-4302. Respondents should be aware that notwithstanding any other provision of law, no person shall be subject to any penalty for failing to comply with a collection of information if it does not display a currently valid OMB control number.</p> <p>PLEASE DO NOT RETURN YOUR FORM TO THE ABOVE ADDRESS.</p>					
1. REPORT DATE (DD-MM-YYYY)		2. REPORT TYPE New Reprint		3. DATES COVERED (From - To) -	
4. TITLE AND SUBTITLE Interactions and Binding Energies of Dimethyl Methylphosphonate and Dimethyl Chlorophosphate with Amorphous Silica			5a. CONTRACT NUMBER W911NF-06-1-0111		
			5b. GRANT NUMBER		
			5c. PROGRAM ELEMENT NUMBER 106013		
6. AUTHORS Joshua Uzarski, Patrick J. Barrie, John R. Morris, Amanda R. Wilmsmeyer			5d. PROJECT NUMBER		
			5e. TASK NUMBER		
			5f. WORK UNIT NUMBER		
7. PERFORMING ORGANIZATION NAMES AND ADDRESSES Virginia Polytechnic Institute & State University Office of Sponsored Programs Virginia Polytechnic Institute and State University Blacksburg, VA 24060 -			8. PERFORMING ORGANIZATION REPORT NUMBER		
9. SPONSORING/MONITORING AGENCY NAME(S) AND ADDRESS(ES) U.S. Army Research Office P.O. Box 12211 Research Triangle Park, NC 27709-2211			10. SPONSOR/MONITOR'S ACRONYM(S) ARO		
			11. SPONSOR/MONITOR'S REPORT NUMBER(S) 49379-CH.6		
12. DISTRIBUTION AVAILABILITY STATEMENT Approved for public release; distribution is unlimited.					
13. SUPPLEMENTARY NOTES The views, opinions and/or findings contained in this report are those of the author(s) and should not be construed as an official Department of the Army position, policy or decision, unless so designated by other documentation.					
14. ABSTRACT The fundamental interactions of dimethyl methylphosphonate (DMMP) and dimethyl chlorophosphate (DMCP) on amorphous silica nanoparticles have been investigated with transmission infrared spectroscopy and temperature-programmed desorption (TPD). DMMP and DMCP both adsorb molecularly to silica through the formation of hydrogen bonds between isolated silanols and the phosphoryl oxygen of the adsorbate. The magnitude of the shift of the $\nu(\text{OH})$ mode upon simulant adsorption is correlated to the adsorption strength. The activation					
15. SUBJECT TERMS DMMP, DMCP, desorption, SiO <sub>2</sub> , TPD, infrared spectroscopy					
16. SECURITY CLASSIFICATION OF:			17. LIMITATION OF ABSTRACT UU	15. NUMBER OF PAGES	19a. NAME OF RESPONSIBLE PERSON John Morris
a. REPORT UU	b. ABSTRACT UU	c. THIS PAGE UU			19b. TELEPHONE NUMBER 540-231-2472

## Report Title

Interactions and Binding Energies of Dimethyl Methylphosphonate and Dimethyl Chlorophosphate with Amorphous Silica

### ABSTRACT

The fundamental interactions of dimethyl methylphosphonate (DMMP) and dimethyl chlorophosphate (DMCP) on amorphous silica nanoparticles have been investigated with transmission infrared spectroscopy and temperature-programmed desorption (TPD). DMMP and DMCP both adsorb molecularly to silica through the formation of hydrogen bonds between isolated silanols and the phosphoryl oxygen of the adsorbate. The magnitude of the shift of the  $\nu(\text{OH})$  mode upon simulant adsorption is correlated to the adsorption strength. The activation energies for desorption for a single DMMP or DMCP molecule from amorphous silica varied with coverage. In the limit of zero coverage, after the effects of defects were excluded, the activation energies were  $54.5 \pm 0.3$  and  $48.4 \pm 1.0$  kJ/mol for DMMP and DMCP, respectively.

---

**REPORT DOCUMENTATION PAGE (SF298)**  
**(Continuation Sheet)**

---

Continuation for Block 13

ARO Report Number     49379.6-CH  
Interactions and Binding Energies of Dimethyl M     ...

Block 13: Supplementary Note

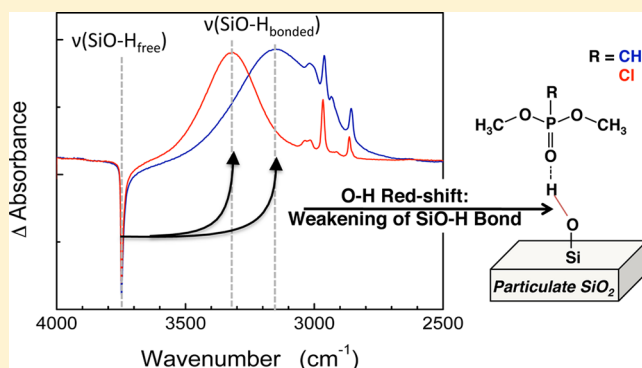
© 2012 . Published in Langmuir, Vol. 28 (30) (2012), ( 30). DoD Components reserve a royalty-free, nonexclusive and irrevocable right to reproduce, publish, or otherwise use the work for Federal purposes, and to authorize others to do so (DODGARS §32.36). The views, opinions and/or findings contained in this report are those of the author(s) and should not be construed as an official Department of the Army position, policy or decision, unless so designated by other documentation.

Approved for public release; distribution is unlimited.

## Interactions and Binding Energies of Dimethyl Methylphosphonate and Dimethyl Chlorophosphate with Amorphous Silica

Amanda R. Wilmsmeyer,<sup>†</sup> Joshua Uzarski,<sup>‡</sup> Patrick J. Barrie,<sup>§</sup> and John R. Morris<sup>\*,†</sup><sup>†</sup>Department of Chemistry, Virginia Tech, Blacksburg, Virginia 24061, United States<sup>‡</sup>U.S. Army Natick Soldier Research, Development, and Engineering Center, Natick, Massachusetts<sup>§</sup>Department of Chemical Engineering and Biotechnology, University of Cambridge, Pembroke Street, Cambridge CB2 3RA, United Kingdom

**ABSTRACT:** The fundamental interactions of dimethyl methylphosphonate (DMMP) and dimethyl chlorophosphate (DMCP) on amorphous silica nanoparticles have been investigated with transmission infrared spectroscopy and temperature-programmed desorption (TPD). DMMP and DMCP both adsorb molecularly to silica through the formation of hydrogen bonds between isolated silanols and the phosphoryl oxygen of the adsorbate. The magnitude of the shift of the  $\nu(\text{OH})$  mode upon simulant adsorption is correlated to the adsorption strength. The activation energies for desorption for a single DMMP or DMCP molecule from amorphous silica varied with coverage. In the limit of zero coverage, after the effects of defects were excluded, the activation energies were  $54.5 \pm 0.3$  and  $48.4 \pm 1.0$  kJ/mol for DMMP and DMCP, respectively.



## 1. INTRODUCTION

Developing a complete understanding of the uptake, bonding, and chemistry of chemical warfare agents (CWAs) on surfaces is critical to the rational design of next-generation sorbents, sensors, and decontamination strategies. To this end, many researchers have performed studies into the surface chemistry of CWA simulants, which are designed to mimic many chemical aspects of agents while lacking their extreme toxicity.<sup>1</sup> However, there are surprisingly few studies that have focused on how structural and chemical differences among simulants affect the resulting chemistry on surfaces, which makes extending simulant results to the actual agents challenging. Therefore, we have begun to explore how small changes in the CWA simulant composition affect interfacial binding on the high-surface-area sorbent, silica.

The uptake and binding of organophosphates (the general class of CWA simulants under investigation here) on surfaces that contain Brønsted-type sites are often dominated by strong hydrogen bond formation.<sup>2–6</sup> In particular, hydrogen bonding of simulants on silica has been previously studied, both experimentally and theoretically.<sup>2–5</sup> Some of the initial studies on this system, performed by Henderson et al., demonstrated that the molecular adsorption of dimethyl methylphosphonate (DMMP) on silica likely proceeds through the formation of hydrogen-bond interactions that may be as high as 71 kJ/mol.<sup>2</sup> Kanan and Tripp extended this work by investigating the adsorption of a series of simulants using IR spectroscopy. Their results suggested that the relative interaction strength of a simulant depends on the number of hydrogen bonds it can

form with the silica surface.<sup>3</sup> Furthermore, they suggested that the strongest simulant–surface interactions occur through hydrogen bonds between the methoxy oxygen atoms of DMMP and surface silanol groups. However, Bermudez employed quantum chemical calculations to show that, for both DMMP and Sarin, adsorption to partially hydroxylated silica more likely occurs through hydrogen bonds between the phosphoryl oxygen and two silanol groups.<sup>4</sup> In exploring possible causes for the inconsistent interpretations of the bonding characteristics for DMMP on silica, Quenneville et al. used molecular dynamics simulations to investigate the interaction of DMMP with amorphous silica as a function of surface hydration.<sup>5</sup> They observed that the surface hydroxyl concentration significantly affected the types of bonds formed between DMMP and the surface. Specifically, they found that, at high hydration levels, hydrogen bonding between the DMMP phosphoryl oxygen and silanols was the dominant interaction pathway but that the DMMP methoxy groups may play a larger role for surfaces with lower hydroxyl densities.

The work described below was designed to provide a quantitative experimental determination of the desorption energies for two simulants, DMMP and dimethyl chlorophosphate (DMCP), on amorphous particulate silica. By tracking the molecule–surface interactions for these two compounds, which differ by a single methyl–chlorine substituent (see

Received: May 11, 2012

Revised: July 3, 2012

Published: July 10, 2012

Figure 1), we aim to provide insight into the fundamental details of interfacial hydrogen bonding. In addition to serving as

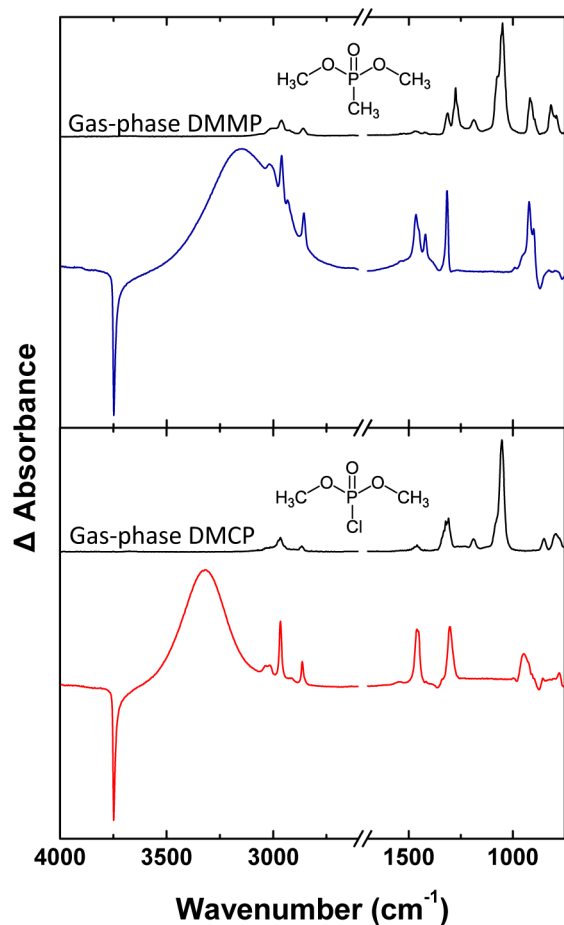


**Figure 1.** Infrared spectra of adsorbed DMMP (top) and DMCP (bottom) on silica.

a needed benchmark for the theoretical studies described above, these results can be used to help predict how halogen substituents within organophosphonates (a key characteristic of the CWAs, Sarin, and Soman<sup>7</sup>) affect the strength of hydrogen bond formation on silica. We have pursued these objectives by performing a series of temperature-programmed desorption (TPD) measurements to determine the activation energy for the desorption of the simulants. In addition, surface-sensitive infrared spectroscopy was utilized to provide insight into how the vibrational modes of the surface and the simulants are affected by adsorption. Through these observations, we have begun to learn about the key functional groups involved in the uptake of the molecules on a silica surface.

## 2. EXPERIMENTAL SECTION

Experiments were performed in an ultra-high vacuum (UHV) chamber with a base pressure of  $10^{-9}$  Torr. The silica sample was prepared by hydraulically pressing approximately 5 mg of Aerosil nanoparticles (200 m<sup>2</sup>/g, 20 nm particle diameter) into a 50- $\mu$ m-thick tungsten mesh grid (Tech-Etch). The sample was resistively heated and cooled, and the surface temperature was monitored with a type-K thermocouple spot-welded to the top of the mesh grid. Immediately prior to experiments, the silica was annealed at 700 K for 5 min to produce a partially dehydroxylated surface. The OH coverage for our sample is estimated to be 2 OH/nm<sup>2</sup>, which is typical for fumed silica under these sample-preparation conditions.<sup>8,9</sup>

DMMP and DMCP were purchased from Sigma and purified via three freeze–pump–thaw cycles prior to use. Simulants were introduced into the UHV system with a directional capillary array doser positioned 2 mm from the silica surface, which was cooled to 225 K. Simulant adsorption on the silica sample was monitored with transmission Fourier transform infrared spectroscopy (FTIR). IR spectra were recorded with a Nicolet Nexus 670 FTIR spectrometer coupled to the UHV instrument. Each spectrum shown below is the compilation of 128 scans collected at 4 cm<sup>-1</sup> resolution with the clean silica sample as the background spectrum. Following simulant exposure, the sample was annealed to 300 and 275 K for the DMMP- and DMCP-saturated samples, respectively. This annealing step was used to provide sufficient mobility for the simulants to diffuse uniformly throughout the particulate sample and as a highly reproducible means to control the surface coverage. In addition, this annealing step eliminates multilayers, enabling the studies to focus on hydrogen bonding between the adsorbates and the surface. For TPD experiments, the surface was heated at a rate of 0.2 K/s and the desorbed species were detected with a doubly differentially pumped Extrel mass spectrometer, which was tuned to the peak of the largest mass fragments for each simulant.

## 3. RESULTS AND DISCUSSION

Previous experimental and theoretical studies have shown that the uptake of DMMP, as well as some chlorinated organophosphates, on the surface of silica occurs through hydrogen bonding to free silanol groups.<sup>2–5</sup> The key infrared spectral signature for hydrogen-bonding interactions between adsorbates and silica is the emergence of a broad SiO–H stretching mode that is red shifted from its original position for the clean surface. Figure 1 shows infrared spectra of partially dehydroxylated SiO<sub>2</sub> particles after the adsorption of either DMMP (top spectrum in blue) or DMCP (bottom spectrum in red). In these spectra, the original bare silica was used as the background such that positive peaks represent new vibrational modes on the surface, and the negative band is due to changes in the frequency of the free SiO–H stretching mode originally present on the surface. The integrated intensity of the broad SiO–H stretching mode caused by hydrogen-bonding interactions is significantly greater than that of the original free SiO–H stretch because of the enhanced oscillator strength expected for most hydrogen-bonding systems.<sup>10</sup> During sample exposure, peak positions were observed to be independent of coverage, providing evidence for a single adsorption geometry.

The spectra for both compounds are very similar, reflecting the similar molecular structure for the two adsorbates. Specifically, Table 1 shows that the low-energy bending and deformation modes for the main functional groups are within  $\sim 10$  cm<sup>-1</sup> of each other for the two adsorbates. In addition, the higher-energy, C–H symmetric, and asymmetric modes are nearly identical for the two species. In contrast to these similarities, the hydrogen-bonded SiO–H modes differ by  $\sim 180$  cm<sup>-1</sup> and show a significant difference in the width of the peak. In both cases, the broad SiO–H mode is indicative of hydrogen bonding between the adsorbate and the surface, but the nature of the hydrogen bond appears to be different for DMMP versus DMCP.

In what is now a classic study, Badger and Bauer were the first to show that the stretching frequency for hydrogen-bonded O–H groups in binary solutions is nearly linearly proportional to the strength of the solvent–solute interactions.<sup>11</sup> Similar relationships have been predicted for organophosphonate adsorption on surfaces of silica and hydroxyl-terminated organic surfaces.<sup>3</sup> From these studies, one would predict, on the basis of the IR spectra from Figure 1, that DMMP adsorbs

**Table 1. Assignments of the IR Peaks for DMMP and DMCP in the Gas-phase and Adsorbed on Silica**

mode	DMMP		DMCP	
	gas <sup>c</sup>	ads	gas <sup>c</sup>	ads
Si(O–H) <sub>free</sub>	<sup>a</sup>	3748	<sup>a</sup>	3748
Si(O–H) <sub>bonded</sub>	<sup>a</sup>	3147	<sup>a</sup>	3324
$\nu_a(\text{CH}_3\text{P})$	3013	3014	<sup>a</sup>	<sup>a</sup>
$\nu_a(\text{CH}_3\text{O})$	2962	2965	2966	2968
$\nu_s(\text{CH}_3\text{P})$	2933	2934	<sup>a</sup>	<sup>a</sup>
$\nu_s(\text{CH}_3\text{O})$	2859	2856	2864	2862
$\delta_a(\text{CH}_3\text{O})$	1468 <sup>d</sup>	1466	1461	1461
$\delta_s(\text{CH}_3\text{O})$	1457	1452	1454	1454
$\delta_a(\text{CH}_3\text{P})$	1424 <sup>d</sup>	1421	<sup>a</sup>	<sup>a</sup>
$\delta_s(\text{CH}_3\text{P})$	1313 <sup>d</sup>	1316	<sup>a</sup>	<sup>a</sup>
$\nu(\text{P=O})$	1275	<sup>b</sup>	1309	1270
$\rho(\text{CH}_3\text{O})$	1188	<sup>b</sup>	1190	<sup>b</sup>
$\nu_a(\text{C–O})$	1074	<sup>b</sup>	<sup>b</sup>	<sup>b</sup>
$\nu_s(\text{C–O})$	1050	<sup>b</sup>	1052	<sup>b</sup>
$\rho(\text{CH}_3\text{P})$	918	925	<sup>a</sup>	<sup>a</sup>

<sup>a</sup>Modes are not present in the molecule. <sup>b</sup>Modes are not observable in our sample. <sup>c</sup>See ref 3. <sup>d</sup>For exceptions, see ref 12. <sup>e</sup>Inferred from ref 3.

more strongly to silica. We have tested this hypothesis through the quantitative determination of the desorption energy for these two molecules.

### 3.1. Temperature-Programmed Desorption of DMMP.

The experimental TPD spectra for various coverages of DMMP on silica are shown by the symbols in Figure 2A. In these spectra, the coverage is defined by the fraction of free SiOH groups that form a hydrogen-bonding complex with the adsorbate, as determined by the change in the infrared absorbance for the free SiOH mode during uptake on the surface. According to this description, a saturated surface (defined here as  $\theta = 1$  ML) corresponds to the removal of every free surface OH group. For each TPD spectrum, the molecules were dosed from an effusive source onto the surface held at  $T_s = 225$  K. Following dosing, the surface sample was heated to 300 K to remove weakly adsorbed molecules and to ensure a uniform distribution of adsorbates throughout the sample.

The TPD spectra at several different relative coverages show that, as the coverage decreases, the desorption peaks shift to higher temperatures and the high-temperature edges of the spectra tend to coincide with one another. These characteristics

suggest that there are a distribution of sites with differing binding energies and that, at the temperatures used in this work, the adsorbate is mobile enough to diffuse to the highest-energy site prior to desorption. In addition, the mass spectrometric cracking pattern for DMMP molecules as they desorb from the surface is identical to that of the parent molecules, which indicates that molecular dissociation is very limited on the surface. This conclusion is supported by the IR data of Figure 1, which shows spectroscopic evidence for molecular adsorption.

An often-employed approach to studying the kinetics of desorption for adsorbates from a surface is inversion analysis of the Polanyi–Wigner equation,<sup>13</sup>

$$-\frac{d\theta}{dt}(\theta, T_s) = \nu(\theta, T_s)e^{-E_d(\theta)/k_B T_s} \theta^n \quad (1)$$

where  $\nu$  is the preexponential factor,  $\theta$  is the coverage,  $T_s$  is the surface temperature,  $k_B$  is the Boltzmann constant,  $n$  is the order for desorption, and  $E_d$  is the activation energy for desorption.<sup>14–16</sup> Zubkov et al. recently demonstrated that this method could be effectively applied to describe the desorption of small molecules from highly porous amorphous ice surfaces in UHV-type measurements, provided that diffusion was sufficiently rapid to ensure a uniform distribution of adsorbates throughout the sample.<sup>16</sup> In their work, the close alignment of the high-temperature edges of TPD spectra at varying coverages, as observed here, showed that the diffusion rate was sufficient to ensure uniform coverage and that the rate-limiting step for desorption was the rupture of the adsorbate–surface bond.

The inversion analysis is accomplished by solving the above equation for the desorption energy (for first-order desorption,  $n = 1$ ).

$$E_d(\theta) = -k_B T_s \ln\left(-\frac{d\theta/dt}{\nu\theta}\right) \quad (2)$$

For the analysis, eq 2 provides the desorption energy,  $E_d$ , as a function of coverage by beginning with an assumed value for the preexponential factor,  $\nu$ , for the highest relative coverage TPD spectrum in Figure 2A. The estimated  $E_d(\theta)$  distribution is then numerically integrated to generate a series of simulated desorption spectra at the lower coverages used in the experiments. The preexponential is then treated as a variational parameter with the objective of minimizing the sum-of-the-

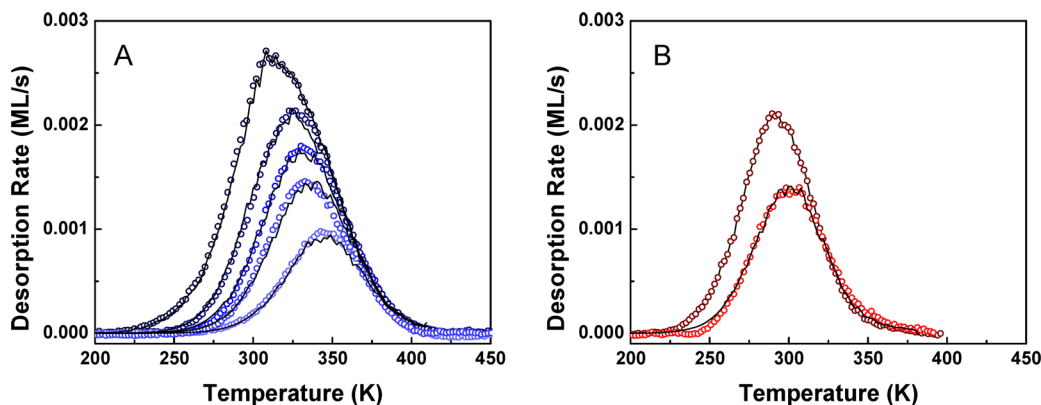


**Figure 2.** (A) TPD of DMMP for a temperature ramp rate of 0.2 K/s. Initial DMMP coverages are 1.0, 0.74, 0.59, 0.47, and 0.28 ML. (B) TPD of DMCP for a temperature ramp rate of 0.2 K/s. Initial DMCP coverages are 0.60 and 0.40 ML. Circles are experimental data, and lines are simulated data obtained from inversion analysis.



squares of the residuals between the simulated TPD spectra and the experimental data.

The solid lines in Figure 2A are the simulated TPD spectra for DMMP desorption from the SiO<sub>2</sub> sample. The simulated spectra agree very well with the experimental data. The excellent fit of the data to the Polanyi–Wigner equation for first-order desorption suggests that this model is valid for describing the desorption kinetics, which can be used to reveal the desorption energy,  $E_d(\theta)$ , and the preexponential factor,  $\nu$ . However, it is well-documented that diffusion and readsorption effects can significantly affect TPD results.<sup>17–22</sup> For TPD from a bed of particles, the observed activation energy can correspond to that for desorption (when readsorption effects are negligible) or can correspond to the heat of adsorption (when readsorption effects dominate). For the case in which adsorption is not an activated process, as is expected to be the case here, these values will be numerically equivalent. Hence, it is believed that reasonably accurate measurements of the binding strength may be obtained from TPD measurements even when readsorption effects occur.<sup>17–21</sup> However, the effect of readsorption means that the value of the pre-exponential factor,  $\nu$ , determined from the TPD experiment is far smaller than would otherwise be expected and it no longer has a simple physical interpretation.<sup>17–21</sup> The prefactor that provides the best fit to the TPD data shown in Figure 2 is  $4.0 \times 10^{6 \pm 0.8} \text{ s}^{-1}$ . This prefactor is significantly smaller than the frequency of a molecular vibration and probably reflects the fact that the molecules desorb and readsorb before reaching the outermost layer of particles and entering the vacuum.<sup>19,20</sup> Therefore, rather than discuss the entropic contributions to the desorption kinetics (information contained within the prefactor) the subsequent discussion focuses on the activation energy, or enthalpic, contribution to desorption.

The  $E_d(\theta)$  curve for DMMP, calculated according to eq 2, that provides the most accurate simulation of the TPD spectra is shown in blue in Figure 3. The broad distribution of desorption energies for the different coverages shown in this curve demonstrates that there are a variety of adsorption sites or molecular geometries. The desorption energies span

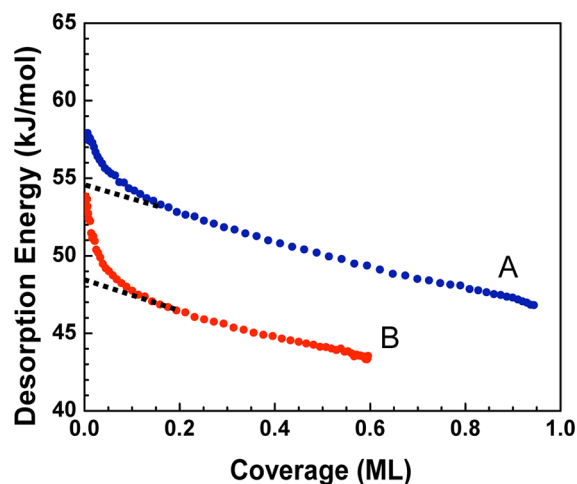


**Figure 3.** Desorption energy as a function of DMMP (A, blue) and DMCP (B, red) coverage. Curves obtained by inversion of the Polanyi–Wigner equation using a prefactor of  $4 \times 10^6 \text{ s}^{-1}$ . Black dotted lines show linear extrapolation to zero coverage. The error bars for replicate runs are within the size of the symbols.

approximately 10 kJ/mol. When the surface hydroxyl groups are nearly saturated with adsorbed DMMP, a fraction of the molecules occupy weak-binding sites, which exhibit the lowest desorption energy of 47 kJ/mol. For very low coverage of DMMP on silica, where the molecules stick preferentially to the highest-energy sites, the desorption energy appears to be as high as 57 kJ/mol. To estimate the desorption energy for a single adsorbate in the absence of high-energy defects, we have extrapolated the linear region of the desorption energy curve to zero coverage (Figure 3). The extrapolation provides a desorption energy in the zero-coverage limit of  $54.5 \pm 0.3 \text{ kJ/mol}$ .

Although spanning a broad range of desorption energies, the values determined in this study are significantly lower than those reported in the recent computational studies of Bermudez.<sup>4</sup> In that work, Bermudez reported the most stable bonding geometry for DMMP on a hydroxylated SiO<sub>2</sub> cluster to be that for which the P=O group forms two hydrogen bonds with adjacent Si–OH groups. This minimum-energy configuration was reported to be bound to the surface by an energy of 88 kJ/mol, which is over 30 kJ/mol higher than the desorption energy for an isolated DMMP molecule as determined from Figure 3. This difference is particularly large, considering that the calculated values do not include energy flow into the molecular degrees of freedom, which should lead to experimentally measured desorption energies that are actually higher than the theoretically derived adsorption energy.<sup>23</sup> However, the surface coverage of hydroxyl groups on the silica sample used in our studies is much lower than that employed in the simulations of Bermudez, which may significantly affect the desorption energy. The density of hydroxyl groups for our silica sample was only  $\sim 2 \text{ OH/nm}^2$ , whereas the calculations employed a density that would be as high as  $4 \text{ OH/nm}^2$  for an extended surface.

The lower surface density of hydrogen-bonding sites likely plays a major role in the average binding energy because there are few surface sites where multiple hydrogen-bonding interactions can occur with the adsorbate. This point was well highlighted in the work of Quenneville and co-workers, which demonstrated that the overall hydrogen-bonding structure of DMMP on amorphous silica depends heavily on the hydroxyl coverage.<sup>5</sup> Their work showed that, at high OH coverage ( $4 \text{ OH/nm}^2$ ), DMMP likely bonds to the surface OH groups through the phosphoryl oxygen ( $\text{P}=\text{O} \cdots \text{HO}-\text{Si}$ ) whereas the structure at lower coverage,  $2 \text{ OH/nm}^2$ , appears to be a combination of phosphoryl-type bonding and hydrogen bonding through the methoxy groups on DMMP. The calculations by Bermudez indicate that the hydrogen-bonding energy for DMMP through the methoxy groups may be 30 kJ/mol lower than bonding through the phosphoryl.

On the basis of these theoretical results, one might speculate that the 54.5 kJ/mol hydrogen-bonding energy between DMMP and silica for the low-surface-density SiO<sub>2</sub> used here is due to interactions between the surface SiOH groups and both the methoxy and phosphoryl parts of the adsorbate. However, significant hydrogen bonding through the methoxy groups should affect the vibrational frequency of key methoxy modes, which does not appear to occur. The IR data indicates that the methoxy-related stretches in the gas phase and on the surface are nearly identical. Therefore, it is unlikely that significant hydrogen bonding occurs between the methoxy groups and the surface.

The above evidence leads to the hypothesis that adsorption is controlled primarily by hydrogen bonding through a single  $\text{P}=\text{O}\cdots\text{HO}-\text{Si}$  attraction. Unfortunately, the phosphoryl stretch is not visible in the IR spectrum for adsorbed DMMP because of the strong spectral overlap of this mode and the  $\text{Si}-\text{O}-\text{Si}$  skeletal vibrations, which block the infrared light over the region from 1300 to 1000  $\text{cm}^{-1}$ . Fortunately, the situation is different for the DMCP simulant, which provides support for the assertion that the primary driving force for adsorption is strong hydrogen-bonding interactions between the phosphoryl group of the adsorbates and silica.

### 3.2. Temperature-Programmed Desorption of DMCP.

Although often used as a simulant for the chemical warfare agent Sarin, DMMP differs from Sarin in a chemically significant way in that it does not contain a phosphorus–halogen bond, which may influence the types and strength of hydrogen-bonding interactions at surfaces. Therefore, we have investigated the desorption of DMCP from silica for comparison to DMMP. The TPD spectra at two coverages for DMCP, on the same silica particles used for DMMP, are shown in Figure 2B. As with DMMP, the excellent fit of the Polanyi–Wigner model to our data (simulation shown by the solid line in Figure 2B) provides confidence that this approach accurately describes the desorption energy. The coverage-dependent desorption energy, derived from the inversion analysis, is provided by the red points in Figure 3.

As revealed in Figures 2 and 3, DMCP is held to the surface much more weakly than DMMP. Clearly, the substitution of a chlorine group in place of a methyl group has a significant effect on the strength of the hydrogen-bonding interactions. The desorption energy for a single DMCP adsorbed to silica is  $48.4 \pm 1$  kJ/mol, approximately 6 kJ/mol lower than that for DMMP. The lower desorption energy is consistent with the qualitative conclusion drawn from analysis of the IR data, which shows a major difference in the extent of the red shift for the hydrogen-bonded  $\text{SiO}-\text{H}$  mode for the two simulants.

The explanation of the different desorption energies for DMMP and DMCP is contained within how the substituent chlorine atom affects the charge distribution within the molecule. The larger electronegativity of the chlorine atom, compared to that of the methyl group, pulls electron density away from the phosphoryl group. Therefore, the partial negative charge on the phosphoryl oxygen atom is likely lower for DMCP than it is for DMMP. The lower negative charge on the phosphoryl oxygen atom for DMCP, relative to that for DMMP, leads to smaller electrostatic interactions with the surface silanol groups.

The hydrogen-bonding interactions through the DMCP phosphoryl group are evidenced by the shift in the  $\text{P}=\text{O}$  mode for this adsorbate relative to that of the gas-phase molecule. The  $\text{P}=\text{O}$  mode for isolated DMCP in the gas phase occurs at 1309  $\text{cm}^{-1}$  (Figure 1 and Table 1). Upon adsorption to silica, this mode shifts by approximately 40  $\text{cm}^{-1}$  whereas all of the other modes for DMCP remain very similar to those of the gas-phase molecule.

Overall, we find that the substitution of a chlorine for a methyl group affects the adsorption strength through hydrogen-bonding-type interactions to surface silanol groups. Furthermore, these studies show that the different bonding energies are clearly reflected in the infrared spectra. The frequency of the hydrogen-bonded  $\text{SiO}-\text{H}$  groups is very sensitive to the strength of the interactions with the phosphoryl oxygen atoms. That is, the  $\text{SiO}-\text{H}$  stretching frequency is 180  $\text{cm}^{-1}$  lower for

DMMP adsorption than for DMCP and the desorption energy is approximately 6 kJ/mol higher for DMMP than for DMCP.

Although the focus of the current work has been on studying the desorption energies and hydrogen-bonding interactions of molecules on particulate silica, further insight into the types of hydrogen bonding that occur may come from TPD experiments performed with single-crystal silica. This approach would limit the utility of infrared spectroscopy but could enable more accurate modeling of this complex system and, as such, the approach presents an opportunity for future work in this area.

Additional future research, recently initiated in our group, will attempt to extend the understanding of how halogen substituents affect relative hydrogen-bonding interactions with surfaces. This work will seek to test a surface analogue to the Badger–Bauer relationship, which states that the OH stretching frequency for solvent–solute interactions scales linearly with the hydrogen-bonding strength. However, the high anharmonicity of the  $\text{SiO}-\text{H}$  stretch may be affected significantly by hydrogen-bonding interactions, which could render the frequency of this stretch only indirectly proportional to bond strength. If the Badger–Bauer relationship does hold for surface adsorbates within hydrogen-bonding systems, then relatively simple infrared measurements over the OH stretching region may provide relative adsorption strengths for molecules on these surfaces without the need for a full temperature-programmed-desorption study.

## AUTHOR INFORMATION

### Notes

The authors declare no competing financial interest.

## ACKNOWLEDGMENTS

The support of the Army Research Office, W911NF-09-1-0150, and the Defense Threat Reduction Agency, W911NF-06-1-0111, is gratefully acknowledged. We thank Professor Diego Troya for many helpful discussions. The authors also thank Z. Dohnálek for a helpful discussion regarding the use of the inversion analysis.

## REFERENCES

- (1) Kim, K.; Tsay, O. G.; Atwood, D. A.; Churchill, D. G. Destruction and Detection of Chemical Warfare Agents. *Chem. Rev.* **2011**, *111*, 5345–5403.
- (2) Henderson, M. A.; Jin, T.; White, J. M. A TPD/AES Study of the Interaction of Dimethyl Methylphosphonate with  $\alpha\text{-Fe}_2\text{O}_3$  and  $\text{SiO}_2$ . *J. Phys. Chem.* **1986**, *90*, 4607–4611.
- (3) Kanan, S. M.; Tripp, C. P. An Infrared Study of Adsorbed Organophosphonates on Silica: A Prefiltering Strategy for the Detection of Nerve Agents on Metal Oxide Sensors. *Langmuir* **2001**, *17*, 2213–2218.
- (4) Bermudez, V. M. Computational Study of the Adsorption of Trichlorophosphate, Dimethyl Methylphosphonate, and Sarin on Amorphous  $\text{SiO}_2$ . *J. Phys. Chem. C* **2007**, *111*, 9314–9323.
- (5) Quenneville, J.; Taylor, R. S.; van Duin, A. C.T. Reactive Molecular Dynamics Studies of DMMP Adsorption and Reactivity on Amorphous Silica Surfaces. *J. Phys. Chem. C* **2010**, *114*, 18894–18902.
- (6) Daly, S. M.; Grassi, M.; Shenoy, D. K.; Ugozzoli, F.; Dalcanele, E. Supramolecular Surface Plasmon Resonance (SPR) Sensors for Organophosphorus Vapor Detection. *J. Mater. Chem.* **2007**, *17*, 1809–1818.
- (7) Yang, Y. C.; Baker, J. A.; Ward, J. R. Decontamination of Chemical Warfare Agents. *Chem. Rev.* **1992**, *92*, 1729–1743.
- (8) Zhuravlev, L. T. Concentration of Hydroxyl Groups on the Surface of Amorphous Silicas. *Langmuir* **1987**, *3*, 316–318.



- (9) Zhuravlev, L. T. The Surface Chemistry of Amorphous Silica. Zhuravlev Model. *Colloids Surf, A* **2000**, *173*, 1–38.
- (10) Tsubomura, H. Nature of the Hydrogen Bond. III. The Measurement of the Infrared Absorption Intensities of Free and Hydrogen-Bonded OH Bands. Theory of the Increase of the Intensity Due to the Hydrogen Bond. *J. Chem. Phys.* **1956**, *24*, 927–931.
- (11) Badger, R. M.; Bauer, S. H. Spectroscopic Studies of the Hydrogen Bond. II. The Shift of the O-H Vibrational Frequency in the Formation of the Hydrogen Bond. *J. Chem. Phys.* **1937**, *5*, 839–851.
- (12) Rusu, C. N.; Yates, J. T. Adsorption and Decomposition of Dimethyl Methylphosphonate on TiO<sub>2</sub>. *J. Phys. Chem. B* **2000**, *104*, 12292–12298.
- (13) Polanyi, M.; Wigner, E. Über die Interferenz von Eigenschwingungen als Ursache von Energieschwankungen und Chemischer Umsetzungen. *Z. Phys. Chem., Abt. A* **1928**, *139*, 439–452.
- (14) Tait, S. L.; Dohnálek, Z.; Campbell, C. T.; Kay, B. D. *n*-Alkanes on MgO(100). I. Coverage-Dependent Desorption Kinetics of *n*-Butane. *J. Chem. Phys.* **2005**, *122*, 164707.
- (15) Zubkov, T.; Smith, R. S.; Engstrom, T. R.; Kay, B. D. Adsorption, Desorption, and Diffusion of Nitrogen in a Model Nanoporous Material. I. Surface Limited Desorption Kinetics in Amorphous Solid Water. *J. Chem. Phys.* **2007**, *127*, 184707.
- (16) Zubkov, T.; Smith, R. S.; Engstrom, T. R.; Kay, B. D. Adsorption, Desorption, and Diffusion of Nitrogen in a Model Nanoporous Material. II. Diffusion Limited Kinetics in Amorphous Solid Water. *J. Chem. Phys.* **2007**, *127*, 184708.
- (17) Palmero, A.; Aldao, C. M. Readsorption and Diffusion-Limited TPD of Water from Zeolite Linde 4A. *Thermochim. Acta* **1998**, *319*, 177–184.
- (18) Palmero, A.; Löffler, D. G. Kinetics of Water Desorption from Pelletized 4A and 5A Zeolites. *Thermochim. Acta* **1990**, *159*, 171–176.
- (19) Gorte, R. J. Design Parameters for Temperature Programmed Desorption from Porous Catalysts. *J. Catal.* **1982**, *75*, 164–174.
- (20) Muhler, M.; Rosowski, F.; Ertl, G. The Dissociative Adsorption of N<sub>2</sub> on a Multiply Promoted Iron Catalyst Used for Ammonia Synthesis: A Temperature Programmed Desorption Study. *Catal. Lett.* **1994**, *24*, 317–331.
- (21) Rieck, J. S.; Bell, A. T. Influence of Adsorption and Mass Transfer Effects on Temperature-Programmed Desorption from Porous Catalysts. *J. Catal.* **1984**, *85*, 143–153.
- (22) Kanervo, J. M.; Keskitalo, T. J.; Slioor, R. I.; Krause, A. O. I. Temperature-Programmed Desorption as a Tool to Extract Quantitative Kinetic or Energetic Information for Porous Catalysts. *J. Catal.* **2006**, *238*, 382–393.
- (23) Taylor, D. E.; Runge, K.; Cory, M. G.; Burns, D. S.; Vasey, J. L.; Hearn, J. D.; Henley, M. V. Binding of Small Molecules to a Silica Surface: Comparing Experimental and Theoretical Results. *J. Phys. Chem. C* **2011**, *115*, 24734–24742.